J. Membrane Biol. 191, 77–86 (2002)
DOI: 10.1007/s00232-002-1045-1

The Journal of
Membrane
Biology

Hepatocyte Growth Factor/Scatter Factor Stimulates Ca^{2+}-Activated Membrane K^+ Current and Migration of MDCK II Cells

M. Jin, D. M. Defoe[1], R. Wondergem
Department of Physiology and [1]Department of Anatomy and Cell Biology, James H. Quillen College of Medicine, East Tennessee State University, PO Box 70,576, Johnson City, TN 37614, USA

Received: 19 April 2002/Revised: 16 August 2002

Abstract. Hepatocyte growth factor/scatter factor (HGF/SF) stimulates migration of various cells and has been linked via Met tyrosine kinase-signaling to transformation and the metastatic phenotype. Migration of transformed MDCK-F cells depends on activation of a charybdotoxin-sensitive, volume-activated membrane K^+ current. Thus, we used patch-clamp electrophysiology and transwell migration assays to determine whether HGF/SF stimulation of MDCK II cell migration depends on the activation of membrane K^+ currents. HGF/SF activated a membrane K^+ current that increased over 24 hr, and which could be modulated by increasing intracellular calcium concentration, $[Ca^{2+}]_i$. Charybdotoxin (ChTX, 50 nM), iberiotoxin (IbTX, 100 nM), stichodactyla toxin (Stk, 100 nM) and clotrimazole (CLT, 1 μM) all inhibited this current. HGF/SF (100 scatter units/ml) significantly increased MDCK II cell migration over 8 hr compared to control cells. Addition of ChTX (50 nM), IbTX (100 nM), Stk (100 nM) or CLT (1 μM) inhibited the HGF/SF-stimulated MDCK II cell migration. We conclude that the activation of membrane Ca^{2+}-activated K^+ current is necessary for HGF/SF stimulation of MDCK II cell.

Key words: Ca^{2+}-activated K^+ channel — Iberiotoxin — Charybdotoxin — Migration assay

Introduction

Hepatocyte growth factor/scatter factor (HGF/SF) is a multifunctional effector of cells expressing the Met tyrosine kinase receptor. In addition to promoting epithelial growth and survival, HGF/SF stimulates dissociation, migration, invasion and morphological changes in various cells (Matsumoto & Nakamura, 1996, 1997; Montesano et al., 1997). In vivo, HGF/SF-Met binding is essential for normal embryological development of the nervous system, kidney, muscle, mammary gland and liver (Matsumoto & Nakamura, 1996, 1997). HGF/SF signaling also is involved in the processes of tissue regeneration and wound healing (Matsumoto & Nakamura, 1997).

The ligand-receptor pair also plays a role in malignancy. The human oncogene, *tpr-met*, encodes an altered Met protein, which has constitutive, ligand-independent tyrosine kinase activity and transforming ability (Jeffers et al., 1996). HGF/SF-Met signaling enhances the in vitro invasiveness and in vivo metastatic potential of tumor cells, such as ras-transformed NIH3T3, C127, and SK-LMS-1 cells (Jeffers et al., 1996; Jeffers, Rong & Vande Woude, 1996a, b). Interruption of HGF/SF-Met signaling shows the possibility for therapeutic intervention to inhibit tumor growth and metastasis. Neutralizing monoclonal antibodies to HGF/SF inhibit HGF/SF-Met signaling in vitro, as well as the growth of a human glioblastoma multiform xenograft in athymic *nu/nu* mice (Cao et al., 2001). Dominant-negative mutants of Met inhibit HGF/SF-Met signaling and cell invasion of ras-transformed cells in vitro, as well as the subcutaneous tumor growth and metastasis in vivo (Furge et al., 2001).

MDCK epithelial cells grow in colonies of tightly associated cells, and these have been used intensively as an in vitro model for HGF/SF-induced cell scattering, migration and tubulogenesis (Terauchi & Kitamura, 2000). Prolonged exposure to an alkaline culture medium transforms MDCK to MDCK-F cells, which dramatically affects cell function and polarization (Schwab & Oberleithner, 1996). MDCK-F cells proliferate and migrate without con-

Correspondence to: R. Wondergem; email: wonderge@etsu.edu

Table 1. Salt solutions used to fill bath and pipet

SOLUTION	Na gluconate (mM)	K gluconate (mM)	$CaCl_2$ (mM)	$MgCl_2$ (mM)	EGTA (mM)	Glucose (mM)	HEPES (mM)	pH
External (bath)	135	5.4	1.8	2	–	10	5	7.41
External (hypo)	95	5.4	1.8	2	–	10	5	7.41
External (high K)	0.4	140	1.8	2	–	10	5	7.41
Internal (7 μM free Ca^{2+})	–	140	0.998	2	1	–	5	7.2
Internal (1 μM free Ca^{2+})	–	140	0.854	2	1	–	5	7.2
Internal (28 nM free Ca^{2+})	–	140	0.1	2	1	–	5	7.2

tact inhibition. In contrast, wild-type MDCK cells only migrate when they lose contact to neighboring cells, and at a much slower speed (Schwab & Oberleithner, 1996). MDCK-F cells also show remarkably altered electrophysiological properties. In brief, intracellular Ca^{2+} activity ($[Ca^{2+}]_i$), membrane conductance and membrane potential fluctuate in MDCK-F cells (Schwab & Oberleithner, 1996; Schwab et al., 1995). Ca^{2+}-activated K^+ channels underlie the oscillation of the membrane potential. Application of K^+ channel blockers, such as barium, tetraethylammonium, 4-aminopyridine and charybdotoxin markedly inhibits cell migration, suggesting the importance of K^+ channels in this process (Schwab et al., 1994). Therefore, in addition to the cytoskeletal 'migration machinery', locomotion of MDCK-F cells depends on the oscillatory activity of Ca^{2+}-activated K^+ channels that are inhibited by ChTX (Schwab & Oberleithner, 1996). HGF/SF also induces an oscillatory Ca^{2+}-activated K^+ current in human gastric carcinoma SC-M1 cells, which is abolished when tetraethylammonium chloride or a low-Ca^{2+} solution is included in the recording pipette (Liu et al., 1998). Similarly, HGF/SF-induced Ca^{2+} oscillation is observed in hepatocytes (Baffy et al., 1992; Osada et al., 1992; Kaneko et al., 1992; Kawanishi et al., 1995).

In the present study, we have used patch-clamp electrophysiology and transwell migration assays to investigate HGF/SF effects on Ca^{2+}-activated membrane K^+ currents and migration of MDCK II cells. Since HGF/SF stimulates the migration of MDCK cells, as well as the metastasis of various tumor cells, we postulate that Ca^{2+}-activated K^+ channels also play a role in the HGF/SF-stimulated migration of MDCK II cells.

Materials and Methods

Cell Culture

Madin-Darby canine kidney epithelial MDCK II cells were maintained in 25-mm^2 T-flasks with Dulbecco's modified Eagle's medium/Ham's F-12 medium (Sigma, St. Louis, MO), which was supplemented with 5% fetal bovine serum (Atlanta Biologicals, Norcross, GA), 100 I.U./ml penicillin, 100 μg/ml streptomycin (Sigma), and equilibrated with 95% air/5% CO_2 in a water-jacketed tissue-culture incubator. Medium was changed every other day, and cells were passaged every 5–7 days. The latter consisted of washing the cells twice with phosphate-buffered saline (PBS), incubating them 45–60 min with porcine trypsin (1.2–2.5 mg/ml PBS), followed by pelleting of the suspended cells, aspirating the trypsin solution, diluting with fresh complete medium, and replating the cells.

Human HGF/SF was obtained as a gift from Drs. G.F. Vande Woude and L.-M. Wang, Van Andel Research Institute, Grand Rapids, MI. HGF/SF concentrations are presented as scatter units/ml; five scatter units are equivalent to approximately 1 ng of protein. Cells for patch clamp were treated with or without HGF/SF for 4 or 24 hr; cells for the transwell migration assay were treated for 8 hr.

Whole-Cell and Cell-attached Voltage-Clamp Technique

Cells were seeded on 4 × 4-mm sections of plastic coverslips for 24 hr before treatment with HGF/SF. After treatment the coverslips were transferred to an acrylic chamber (Warner, New Haven, CT) on the stage of an inverted microscope (Olympus IMT-2, Melville, NY) equipped with Hoffman modulation contrast optics. Cells were superfused at room temperature with a standard external salt solution, and gluconate was used to substitute for the Cl^- in the solution. The composition of this solution and other solutions used throughout these experiments are given in Table 1. For cell-attached patch clamp, pipettes were filled with standard external gluconate solution. For whole-cell patch clamp, pipettes were filled with standard internal gluconate solution, which was buffered with EGTA to reach a free Ca^{2+} concentration of 28 nM, 1 μM or 7 μM according to Prof. G. Droogmans (ftp://ftp.cc.kuleuven.ac.be/pub/droogmans/cabuf.zip).

Borosilicate glass capillaries (1.2 mm OD, 0.68 ID, type EN-1, Garner Glass, Claremont, CA) were cleaned in a sonicator and dried in a convection oven at 90°C. Pipettes (3–8 MΩ in the bath solution) were fabricated from the capillaries with a Brown-Flaming horizontal micropipette puller (P-87, Sutter Instruments, San Rafael, CA). Whole-cell pipettes were coated to within 0.5 mm of the tip with polystyrene base coil dope (Polyweld 912, Amphenol, Wallingford, CT). Cell-attached pipettes to record channel currents were coated with R6101 (Dow Corning, Midland, MI) to reduce the noise (Rae & Levis, 2000). The tips were heat-polished prior to use. A micromanipulator (MO-202, Narishige, Tokyo) fixed to the microscope was used to position pipettes.

The whole-cell and cell-attached configurations were obtained by standard patch-clamp technique (Hamill et al., 1981). Membrane currents were measured with a patch-clamp amplifier (Axopatch 1-D, Axon Instruments, Foster City, CA) with the low-pass, Bessell filtering (−3 dB) set at 2 kHz. Whole-cell currents from the patch-clamp amplifier were fed into a DMA-1 digital interface connected to a 486-SX computer equipped with Clampex software (Axon Instruments). Records were stored on an internal Jaz drive (Iomega, Roy, UT). Ag/AgCl half-cells constituted the electrodes,

and an agar bridge (4% w/v in external gluconate solution) connected the reference electrode to the bath solution. The junction null was zeroed in the cell-attached mode prior to whole-cell access. Electrode series resistance was measured following whole-cell access, and it was compensated prior to recording.

Transwell Cell Migration Assay

Transwell polycarbonate membranes with a pore size of 8 μm were inserted into 24-well cluster plates (Costar, Cambridge, MA). The bottom side of each membrane was coated with 100 μl of fibronectin (25 μg/ml in sterile PBS; Sigma). These were rinsed twice with PBS, once with 1% bovine serum albumin (BSA; Sigma) in PBS, and blocked with 1% BSA in PBS for 30 min at room temperature. The bottom side of each control membrane was treated with 100 μl BSA (1% in PBS) for 1 hr at room temperature. 800 μl of migration assay buffer (containing serum-free DMEM/F-12, 0.1% BSA, 100 I.U./ml penicillin, 100 μg/ml streptomycin) were added to the lower chamber of each well. HGF/SF, charybdotoxin (ChTX), iberiotoxin (IbTX), stichodactyla toxin (Stk) (Alomone Laboratories, Jerusalem, Israel, and Accurate Chemical & Scientific Corporation, Westbury, NY), clotrimazole (CLT) (Sigma) and combinations were added to the lower chambers before moving the inserts into the wells. The final concentration of these drugs was computed by assuming diffusion equilibration with the 200-μl volume of medium added to the upper chambers. MDCK II cells were harvested, washed in PBS, and suspended in migration assay buffer at a cell density of 300,000 cells/ml. 200-μl aliquots of cells were plated on the upper membrane surface of each insert. The tissue culture plates were then returned to the tissue-culture incubator for 8 hr. Inserts were rinsed, and cells on the upper membrane surface were gently removed using cotton swabs. Cells on the under surface were fixed in 100% methanol (10 min) at 4°C and stained for 15 min with modified Harris hematoxylin solution (Sigma). Ten randomly selected fields of 0.6 mm^2 were counted, using an inverted microscope (Olympus IMT-2, Melville, NY) to determine the number of cells that had migrated in the experimental groups and the untreated controls. Each experiment was repeated three times.

Statistics

Results are given as mean ± SEM. One-way analysis of variance, multiple comparisons and regression analysis were performed where applicable. Analyses of covariance and *t*-test were performed to compare slope conductance. Significant differences among means or slopes were determined at $P < 0.05$.

Results

Effects of HGF/SF on Membrane K^+ Currents in MDCK II Cells

MDCK II cells formed discrete colonies of tightly juxtaposed cells when seeded on coverslips. HGF/SF (100 scatterunits for 8 & 24 hr) polarized the morphology in many cells, which included the lamellipodia and trailing cell body that characterized migrating cells. The cells also were readily studied by patch-clamp electrophysiology.

Whole-cell recordings were performed to determine whether HGF/SF activated membrane ion currents. The recording parameters in this regard were: the pipette/membrane seal resistance = 5.8 ± 0.2 GΩ (n = 112), the whole-cell capacitance = 16.8 ± 0.7 pF, the series access resistance = 7.2 ± 0.2 MΩ, and the whole-cell resistance = 170 ± MΩ (with 1 μM free Ca^{2+} in the pipette internal solution). A representative trace of whole-cell current, which was recorded in response to voltage steps applied from −100 to 80 mV to an HGF/SF-treated cell (200 scatter units for 24 hr), is shown in Fig. 1*A*. Current-voltage (*I-V*) relationships, which were obtained from data points taken at the end of similar voltage pulses, yielded continuous increases in membrane conductance at 4 and 24 hr of HGF/SF treatment compared with control cells, Fig. 1*B*. Voltage ramps from −100 to 100 mV also were applied to an HGF/SF-treated cell (200 scatter units/ml for 24 hr), Fig. 1*C*. This was done first under control conditions of 5.4 mM external $[K^+]$; then the voltage ramp was repeated after the cell was exposed to 140 mM external $[K^+]$, which was symmetrical with the pipette $[K^+]$; and then after switching back to control solution. The increase in external $[K^+]$ resulted in a shift in current reversal potential from ≈ −60 mV to ≈ 5 mV, along with an increase in slope conductance. These reversed after switching back to the control solution. Such responses of the HGF/SF-treated cell to the changes in external $[K^+]$ were consistent with those expected of membrane K^+ conductance.

Effects of ChTX, IbTX, Stk and CLT on HGF/SF-Stimulated Membrane K^+ Currents

Various inhibitors of Ca^{2+}-activated K^+ channels were utilized to determine whether HGF/SF stimulation of membrane K^+ current may have resulted from activity of these channels. ChTX (50 nM for 5 min) inhibited membrane K^+ current in MDCK II cells that were treated with HGF/SF (200 scatter units/ml for 24 hr), Fig. 1*A*. The *I-V* plots in Fig. 2 comprise summary results from repeated measurements as shown in Fig. 1*A*. ChTX had no significant effect on slope conductance for K^+ currents in untreated control MDCK II cells (ANCOVA, $P > 0.05$, n = 7 cells), Fig. 2*A*. HGF/SF at 200 scatter units/ml significantly increased slope conductance of membrane K^+ current, which was inhibited by added ChTX at 50 nM (ANCOVA, $P < 0.05$, n = 7 cells), Fig. 2*B*. IbTX also inhibited HGF/SF-stimulated membrane K^+ currents in MDCK II cells. IbTX at 100 nM significantly decreased slope conductance of membrane K^+ current (ANCOVA, $P < 0.05$, n = 4 cells), along with a modest shift in reversal potential toward 0 mV in MDCK II cells treated for 24 hr with 200 scatter units/ml of HGF/SF, Fig. 2*C*. CLT (1 μM) had no effect on HGF/SF-stimulated (200 scatter units/ml, for 24 hr) membrane K^+ current in MDCK II cells dialyzed with 1 μM $[Ca^{2+}]_i$. The slope con-

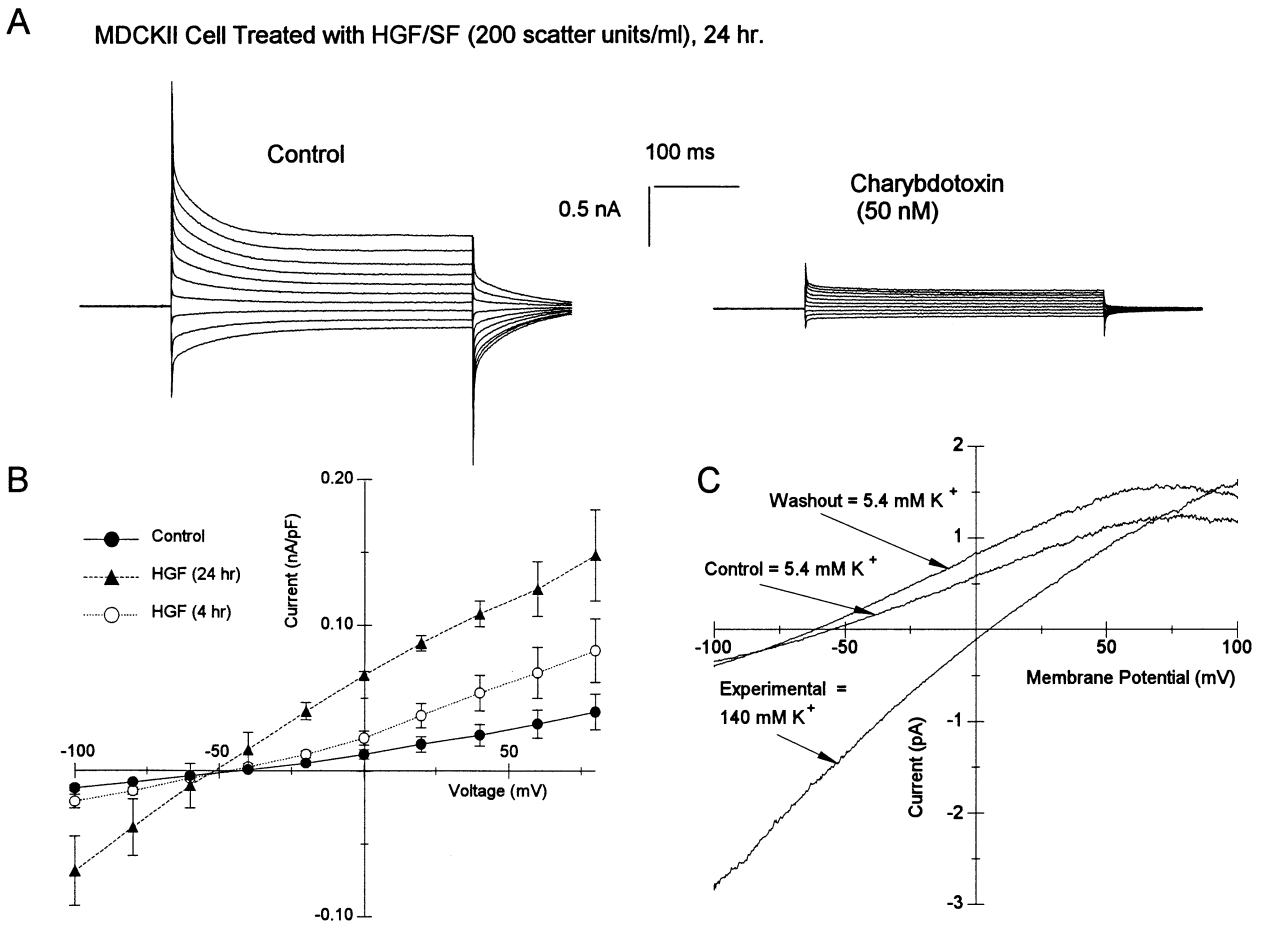

Fig. 1. Whole-cell currents in MDCK II cells. (*A*) Effect of K^+ channel blocker ChTX on HGF/SF-stimulated membrane K^+ current in an MDCK II cell. Whole-cell currents were recorded during voltage pulses that ranged from −100 to 80 mV in consecutive, 20-mV increments. Holding potential = −50 mV. *Left*. MDCK II cell treated with 200 scatter units/ml HGF/SF for 24 hr in standard external solution with gluconate. *Right*. The same cell 5 min after 50 nM ChTX in the external solution. (*B*) Effects of HGF/SF on membrane K^+ currents in MDCK II cells after 4 and 24 hr (200 scatter units/ml HGF/SF). Current-voltage (*I-V*) plots for whole-cell currents recorded in MDCK II cells during voltage pulses ranging from −100 to 80 mV in consecutive, 20-mV increments (mean ± SE; $n = 3$ cells). (*C*) Whole-cell currents recorded in a MDCK II cell on application of voltage ramps from −100 to 100 mV (1.5 sec in duration). Control trace was recorded right after break-in, experimental trace was recorded shortly after exchange of extracellular solution with 140 mM K^+ from a solution containing only 5.4 mM K^+ (Control). Washout trace was recorded after switching back to control solution.

ductance of the treated cells was 0.62 ±0.18 nS/pF ($n = 3$). This decreased to 0.30 ± 0.07 nS/pF ($n = 3$) with 1 μM CLT; however, the difference was not significant ($P > 0.05$). Stk (100 nM) also had no effect on HGF/SF-stimulated (200 scatter units/ml for 24 hr) membrane K^+ current (*data not shown*).

To characterize further the HGF/SF stimulation of membrane K^+ current in MDCK II cells, the inhibitor experiments were repeated at 7 μM internal $[Ca^{2+}]$, a concentration that was sufficient for the activation of all types of Ca^{2+}-activated K^+ channels (Hille, 2001). Whole-cell current traces are shown in Fig. 3*A* for comparison with those obtained from cells dialyzed with 1 μM $[Ca^{2+}]_i$, Fig. 1*A*. Membrane currents were greater at all voltages compared with measurements made with 1 μM internal $[Ca^{2+}]_i$, and the corresponding *I-V* curves rectified inwardly, Fig. 3*B–F*. Moreover, HGF/SF treatment (50 scatterunits/ml for 24 hr) stimulated membrane current at near zero mV and at positive membrane potentials, Fig. 3*B*. K^+ channel inhibitors added for 5 min significantly reduced slope conductance of the whole-cell current in HGF/SF-stimulated cells (ChTX, Fig. 3*C*, IbTX, Fig. 3*D*, Stk, Fig. 3*E* and CLT, Fig. 3*F*). All these inhibitors, except CLT, also significantly reduced the reversal potential. ChTX (50 nM) also significantly reduced slope conductance and reversal potential of the whole-cell K^+ current in untreated MDCK II cells (*not shown*); however, CLT had no effect.

The difference currents obtained from results shown in Fig. 3 were plotted as a function of voltage for all inhibitors (Fig. 4). Here, the ordinate comprises the control currents minus the currents obtained following addition of each inhibitor. These currents were

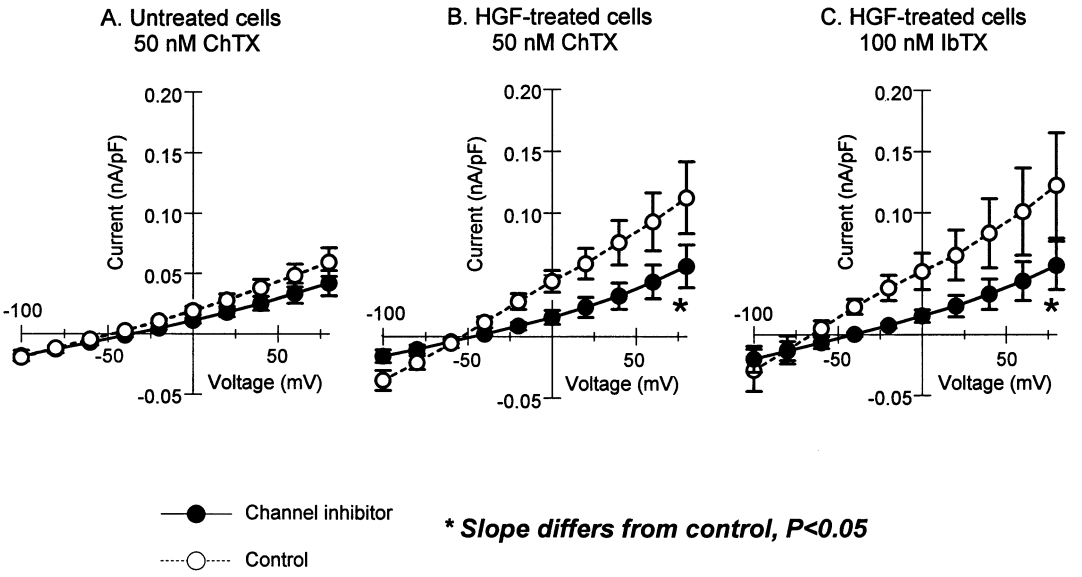

Fig. 2. Inhibitory effects of ChTX and IbTX on HGF/SF-stimulated membrane K^+ currents in MDCK II cells. $[Ca^{2+}]_i$ was buffered to 1 μM. MDCK II cells were untreated or treated with 200 scatter units/ml HGF/SF for 24 hr. Current-voltage (*I-V*) plots for whole-cell currents recorded from −100 to 80 mV (100 msec) in consecutive, 20-mV increments. Holding potential = −50 mV. (*A*) Effect of 50 nM ChTX on untreated MDCK II cells (n = 7). (*B*) Effect of 50 nM ChTX on HGF/SF-treated MDCK II cells (n = 7). (*C*) Effect of 100 nM IbTX on HGF/SF-treated MDCK II cells (n = 4). There is a significant difference between the slope conductance in control solution and in a solution with channel inhibitor (mean ± SE; $P < 0.05$).

Table 2. Effects of intracellular $[Ca^{2+}]$ on slope conductance and reversal potential (V_r) of *I-V* plots measured in untreated and HGF/SF-treated MDCK cells in both absence and presence of charybdotoxin (ChTX, 50 nM).

Internal $[Ca^{2+}]_i$	Bath solution	Untreated		HGF/SF-treated	
		Slope (nA/pF)	V_r (mV)	Slope	V_r (mV)
28 nM[a]	Control	0.24 ± 0.04 (n = 4)	−55.9 ± 18.0 (n = 4)	0.32 ± 0.08 (n = 3)	−71.1 ± 10.9 (n = 3)
	ChTX	0.23 ± 0.05 (n = 4)	−60.6 ± 21.2 (n = 4)	0.26 ± 0.09 (n = 3)	−64.3 ± 14.5 (n = 3)
1 μM[a]	Control	0.38 ± 0.05 (n = 7)	−47.6 ± 3.5 (n = 7)	0.79 ± 0.15 (n = 7)[c]	−52.1 ± 4.5 (n = 7)
	ChTX	0.29 ± 0.06 (n = 7)	−35.8 ± 4.1 (n = 7)	0.30 ± 0.10 (n = 7)[d]	−44.7 ± 3.8 (n = 7)
7 μM[b]	Control	0.90 ± 0.09 (n = 5)	−100 ± 4.9 (n = 5)	0.93 ± 0.16 (n = 5)	−101.2 ± 3.5 (n = 5)
	ChTX	0.37 ± 0.09 (n = 5)[d]	−76.8 ± 7.6 (n = 5)[d]	0.33 ± 0.08 (n = 6)[d]	−70.8 ± 6.9 (n = 6)[d]

[a] For $[Ca^{2+}]_i$ of 28 nM and 1 μM, HGF/SF-treated MDCK cells were treated with 200 scatter units/ml HGF/SF for 24 hr.
[b] For $[Ca^{2+}]_i$ of 7 μM, HGF/SF-treated MDCK cells were treated with 50 scatter units/ml HGF/SF for 24 hr.
[c] Differs from the corresponding measurement in untreated cells, $P < 0.05$.
[d] Differs from the corresponding measurement in control solution, $P < 0.05$.

voltage-dependent in a manner consistent with either inward rectification or current inactivation at positive membrane potentials, or perhaps both. Moreover, the actual and extrapolated reversal potentials were in fair agreement, yet more negative than the predicted K^+ equilibrium potential of −84 mV.

Whole-cell recordings were also performed under conditions of minimal $[Ca^{2+}]_i$ at 28 nM. Measurements were done in untreated and HGF/SF-treated cells (200 scatter units/ml) and in the absence or presence of ChTX (50 nM). Summary results consisting of slope conductances and reversal potentials are shown in Table 2 for all treatment groups. Moreover, summary results from the preceding experiments with either 1 μM or 7 μM internal $[Ca^{2+}]$ also were included in Table 2 for comparison. Membrane slope conductance was lowest at 28 nM $[Ca^{2+}]_i$, and added HGF/SF had no stimulatory effect. Moreover, addition of ChTX resulted in no significant inhibition in either group (Table 2). In contrast, HGF/SF markedly

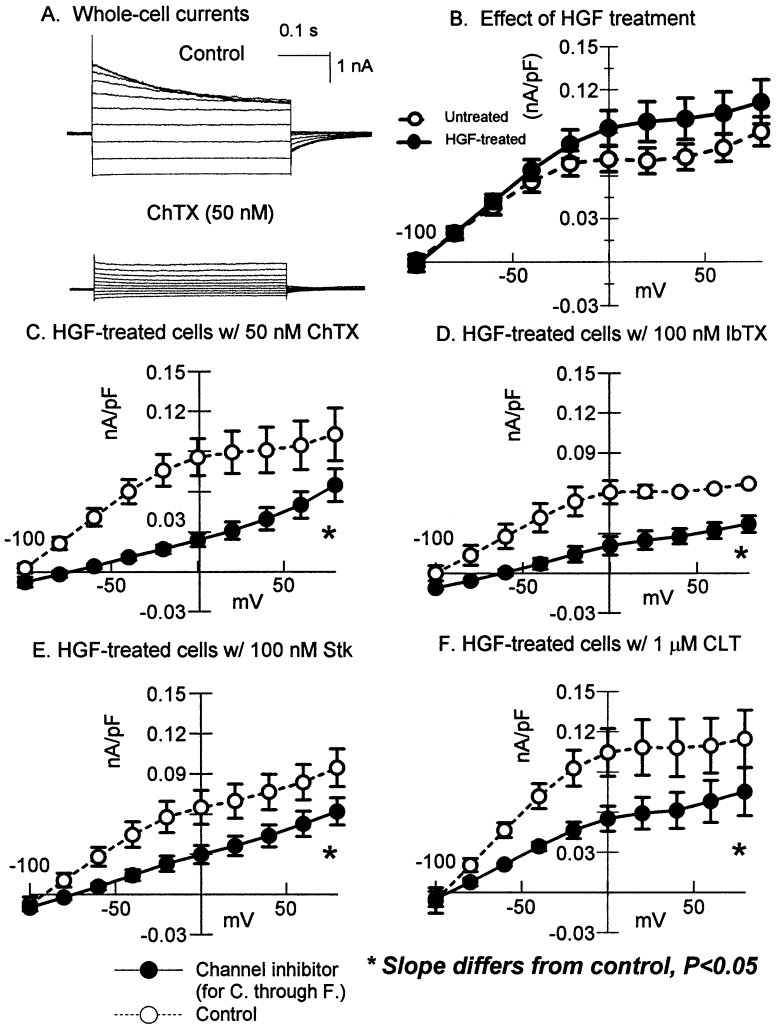

Fig. 3. Effects of HGF/SF on whole-cell currents measured in MDCK II cells. $[Ca^{2+}]_i$ was buffered to 7 μM. (*A*) (*Top*) Representative current traces obtained from whole-cell voltage-clamped MDCK II cell treated for 24 hr with 50 scatterunits/ml HGF/SF. (*Bottom*) Same cell 5 min after superfusing cell with 50 nM ChTX. Voltage pulses ranged from −100 to 80 mV in consecutive, 20-mV increments. Holding potential = −50 mV. (*B*) Current-voltage (*I-V*) plots of currents recorded at the end of the voltage pulses. HGF/SF treatment was 50 scatterunits/ml for 25 hr. Each point is mean ± SE, $n = 9$. (*C–F*) Effects of ChTX (*C*), 50 nM, n_= 5; IbTX (*D*), 100 nM, $n = 3$; Stk (*E*), 100 nM, $n = 6$; and CLT (*F*), 1 μM, $n = 4$, on HGF/SF-stimulated membrane K^+ current in MDCK II cells. $[Ca^{2+}]_i$ was buffered to 7 μM. MDCK II cells were treated with 50 scatter units/ml HGF/SF for 24 hr. *There was significant difference between the slope conductance in control solution and in a solution with channel inhibitor (mean ± SE; $P < 0.05$).

stimulated slope conductance at 1 μM $[Ca^{2+}]_i$, and this was inhibited by ChTX. $[Ca^{2+}]_i$ at 7 μM alone resulted in significant increase in slope conductance, which was inhibited by ChTX along with reduction in the reversal potential. HGF/SF did not increase slope conductance at 7 μM $[Ca^{2+}]_i$; however, as indicated above, currents at positive potentials were greater in the treated cells, Fig. 3*B*.

Effects of HGF/SF, ChTX and IbTX on MDCK II Cell Migration

HGF/SF stimulated MDCK II cell migration in a dose-dependent manner (Fig. 5*A*). Maximum stimulation occurred at 50 scatter units/ml of HGF/SF (8 hr), with no further increases at higher concentrations. ChTX (50 nM) significantly inhibited stimulation of MDCK II cell migration by HGF/SF at 100 scatter units/ml ($P < 0.05$; $n = 3$), Fig. 5*B*. In addition, CLT (1 μM) and Stk (100 nM) both significantly inhibited MDCK II cell migration stimulated by HGF/SF at 100 scatter units/ml for 8 hr, Fig. 5*C*. The inhibition by ChTX also increased with dose (Fig. 6). Here, 25 scatter units/ml of HGF/SF stimulated MDCK II cell migration, and this was inhibited with increasing concentrations of ChTX. However, 100 nM ChTX was necessary for significant inhibition of this submaximal stimulation by HGF/SF (Fig. 6) IbTX (100 nM) also significantly inhibited migration in MDCK II cells treated with 25 scatter units/ml HGF/SF ($P < 0.05$, $n = 3$) (Fig. 6).

To rule out the possibility that HGF/SF stimulation of MDCK II cell proliferation might have accounted for the apparent effects on cell migration, MDCK II cells were plated at 2×10^5 cells per 35-mm tissue-culture dish and allowed to attach for 4 hr. Afterwards, medium was changed to migration assay buffer for a 24-hr equlibration. HGF/SF (100 scatterunits/ml) was then added to five plates for 8 hr, with five additional plates serving as untreated control. Cells were trypsinized and counted in a hemocytometer. The number of cells in untreated control

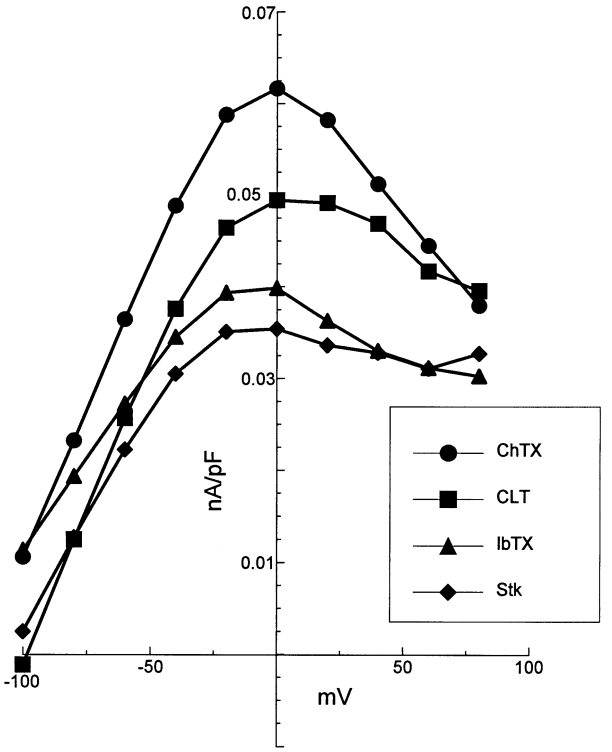

Fig. 4. *I-V* plots of difference currents obtained from HGF/SF-treated MDCK II cells. Values for specific current (nA/pF on the ordinate) were obtained by subtracting currents obtained after inhibitor addition from the corresponding control values shown in Fig. 3*C–F*, respectively.

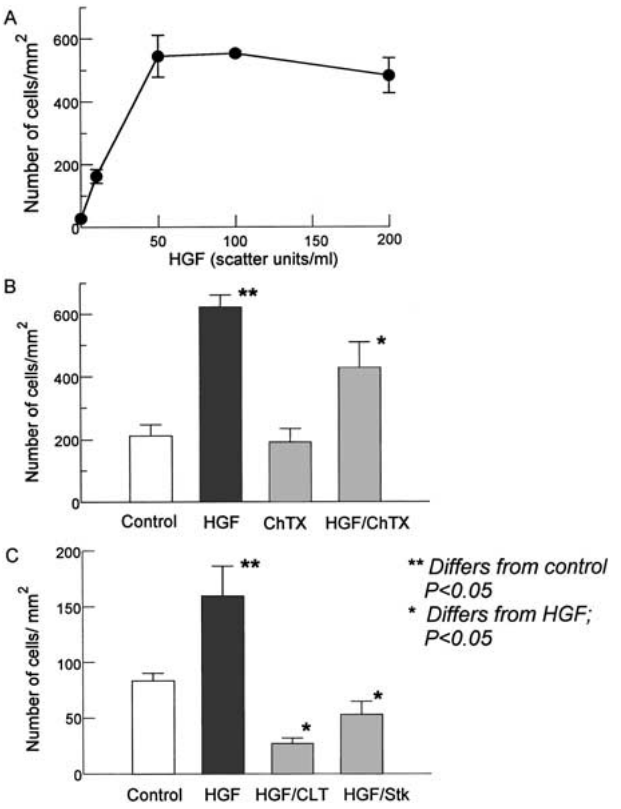

Fig. 5. (*A*) Effects of HGF/SF on MDCK II cell migration in transwell assays. MDCK II cells treated with different concentrations of HGF/SF for 8 hr (mean ± SE; $n = 3$ inserts). (*B*) Effect of K^+ channel blocker ChTX on HGF/SF-stimulated MDCK II cell migration. MDCK II cells were treated with 50 nM ChTX and/or 100 scatter units/ml HGF/SF for 8 hr (mean ± SE; $n = 3$ inserts). (*C*) Effects of CLT and Stk on HGF/SF-stimulated MDCK II cell migration. MDCK II cells were treated with 100 scatter units/ml HGF/SF alone, or with both HGF/SF and a channel inhibitor for 8 hr (mean ± SE; $n = 3$ inserts).

dishes [$1.8 \pm 0.3 \times 10^5$ cells/dish] did not differ ($P > 0.05$; $n = 5$) from the number of cells in dishes with added HGF/SF [$1.9 \pm 0.1 \times 10^5$ cells/dish].

Discussion

We have demonstrated that HGF/SF stimulates cell migration, as well as membrane K^+ currents in MDCK II cells. We also have shown that various agents that block Ca^{2+}-activated K^+ channels, the peptides ChTX, IbTX and Stk along with CLT, inhibit both HGF/SF-stimulated cell migration and membrane K^+ current. CLT is a small molecule with greater lipid solubility compared with the peptide inhibitors, which presumably do not enter the cells or at least at a much slower rate. Therefore, secondary effects of clotrimazole may account for its marked inhibition of migration. Taken together, however, these findings indicate that the activation of Ca^{2+}-activated K^+ channels is necessary for HGF/SF stimulation of MDCK II cell migration.

Schwab and colleagues have demonstrated that the intermediate-conductance Ca^{2+}-activated K^+ channel, IK, plays a role in the migration of the alkaline-transformed MDCK-F cells (Schwab et al., 1993, 1994). Thus, our present findings extend previous work by elucidating the mechanisms through which HGF/SF effects the malignant transformation and the metastatic phenotype (Jeffers et al., 1996, 1996a, b). HGF/SF-Met signaling has been shown to enhance the in vitro invasiveness and in vivo metastasis of tumor cells, such as ras-transformed NIH3T3, C127, and SK-LMS-1 cells (Jeffers et al., 1996, 1996a, b). HGF/SF promotes cell invasion by increasing integrin avidity through Ras activation (Trusolino et al., 2000). Phosphatidylinositol 3-kinase (PI3-kinase) activation following HGF/SF stimulation induces redistribution of junctional complex proteins, such as E-cadherin, desmoplakins and ZO-1, which in turn induces cell dissociation and scattering (Royal & Park, 1995; Khwaja et al., 1998). Homophilic N-cadherin binding between adhering cells plays an important role in maintaining Ca^{2+} homeostasis. HGF/SF induces sustained elevation of $[Ca^{2+}]_i$ in rat ovarian surface epithelial cells in part by its ability to decrease cell contact (Peluso, 1997; Gulati & Peluso, 1997).

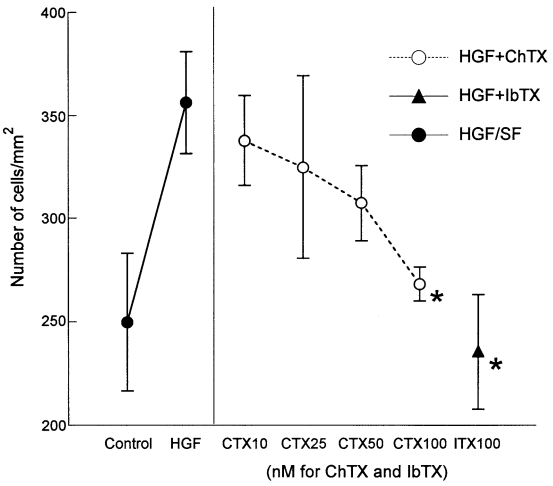

Fig. 6. Effects of ChTX and IbTX on migration of MDCK II cells treated with 25 scatter units/ml HGF/SF. MDCK II cells were treated with HGF/SF and ChTX or IbTX for 8 hr. Statistically significant differences existed between cells treated with 25 scatter units/ml HGF alone and cells treated with 25 scatter units/ml HGF + 100 nM ChTX, or 25 scatter units/ml HGF + 100 nM IbTX (mean ± SE; $n = 3$ inserts).

The doses of HGF/SF that stimulate MDCK migration agree well with the doses that stimulate outward-current channel activity using on-cell patch recording. Larger HGF/SF doses (200 scatterunits/ml) are necessary to activate whole-cell K^+ current when the cells are dialyzed with 1 μM Ca^{2+}. Yet, this large dose of HGF/SF was without effect on membrane K^+ current at 28 nM $[Ca^{2+}]_i$. However, 50 scatterunits/ml effectively stimulate K^+ current at positive membrane potential when the cells are dialyzed with 7 μM Ca^{2+}. Moreover, the Ca^{2+}-activated K^+ channel blockers that inhibit HGF/SF-stimulated MDCK II cell migration also inhibit these whole-cell K^+currents. Taken together, these findings suggest interplay between intracellular Ca^{2+} activation of membrane K^+ currents and the migration of MDCK cells.

The intracellular $[Ca^{2+}]_i$ needed for HGF/SF activation of membrane K^+ current in MDCK II cells is high by physiological standards. Notwithstanding, the intermediate conductance, IK, and the high conductance, BK, Ca^{2+}-activated K^+ channels are thought to be differentially sensitive to $[Ca^{2+}]_i$ with submicromolar amounts needed for IK and micromolar concentrations needed for BK (Hille, 2001). We have no basis to favor either IK or BK in accounting for HGF/SF stimulation of either migration or membrane K^+ current, since inhibitors considered to be quite specific for the respective channels inhibited both variables. However, *I-V* plots of the difference currents (control minus inhibitor) in HGF/SF-treated cells all rectified inwardly. This is of interest, since the currents of cloned, human intermediate-conductance Ca^{2+}-activated K^+ channels expressed in heterologous systems also rectify inwardly (Ishii et al., 1997; Jensen et al., 1998). Whether this is simply coincident or functionally significant requires much more investigation. Nevertheless, we explain the relatively high $[Ca^{2+}]_i$ needed for HGF/SF's stimulation of K^+ current by the physiological kinetics of Ca^{2+}-activated K^+ current, which includes the diverse parameters that regulate intracellular $[Ca^{2+}]_i$ and the degree of colocalization of $K_{(Ca)}$ channels and the intracellular sites of elevated $[Ca^{2+}]_i$.

HGF/SF causes oscillations of calcium activity in hepatocytes (Baffy et al., 1992; Osada et al., 1992; Kaneko et al., 1992; Kawanishi et al., 1995) and oscillations of Ca^{2+}-activated K^+ current in human gastric cancer cells (Liu et al., 1998). In this regard, migration of MDCK-F cells depends on a charybdotoxin-sensitive oscillation of Ca^{2+}-sensitive 53-pS K^+ channels (Schwab et al., 1994). Oscillations of intracellular $[Ca^{2+}]_i$ trigger opening of these channels, which result in oscillations of membrane potential (Schwab & Oberleithner, 1996). Moreover, migrating MDCK-F cells demonstrate a horizontal gradient for intracellular $[Ca^{2+}]_i$ with oscillations of $[Ca^{2+}]_i$ being greater in the cell body than in the lamellipodium (Schwab et al., 1997).

Gradients and oscillations of intracellular $[Ca^{2+}]_i$ have been associated with local Ca^{2+} signaling called "puffs" in nonexcitable cells and "sparks" in excitable cells. These constitute cytoplasmic Ca^{2+} microdomains that control local, apical secretion in acinar cells (Kidd et al., 1999), neurotransmitter release (Neher, 1998), or neuronal growth (Spitzer et al., 2000), or they may coalesce to form an intracellular Ca^{2+} wave that leads to myocyte contraction (Bootman, Lipp & Berridge, 2001). In smooth muscle, Ca^{2+} sparks activate BK channels in the membrane microdomain that regulate membrane potential and voltage-gated channels (Zhuge et al., 2000; Pérez, Bonev & Nelson, 2001; Pozo et al., 2002). In a similar manner, migrating MDCK-F cells are polarized cells that rely on Ca^{2+}-activated K^+ (IK) channels, which are more active in the rear of the cells (Schwab et al., 1995) and are associated with the larger of the Ca^{2+} transients (Schwab et al., 1997). Moreover, topical application of charybdotoxin to the cell body inhibits MDCK-F cell migration (Schwab et al., 1997) and results in cell swelling (Schneider et al., 2000), whereas topical application of ionomycin to the cell body shrinks the cells (Schneider et al., 2000).

Ca^{2+}-activated K^+ channels are critical to regulatory volume decrease (RVD) in many cell types (Pasantes-Morales & Morales-Mulia, 2000). Migrating cells are polarized with K^+ efflux-dependent cell shrinkage occurring in the rear of the cells to facilitate retreat (Schwab, 2001). In contrast, gelosmotic swelling occurs in the lamellipodium, providing membrane tension necessary to advance the cell mi-

gration (Schwab, 2001). It has been proposed that ion channels and transporters modulate cytoskeletal migration machinery by regulating $[Ca^{2+}]_i$ and local cell volume of migrating cells (Schneider et al., 2000). Human melanoma cells that are devoid of the actin cross-linking protein ABP280 are unable to volume-regulate or activate K^+ channels when exposed to a hypotonic stimulus. After transfection with ABP280, these cells could migrate as well as regulate K^+ channels (Cantiello et al., 1993). However, migration of rescued melanoma cells is inhibited when Ca^{2+}-activated K^+ channels are blocked (Cantiello et al., 1993).

In summary, HGF/SF is a multifunctional effector that stimulates morphological changes, dissociation, scatter and migration of epithelial and other cell types. ChTX, IbTX, Stk, and CLT all inhibit HGF/SF-stimulated membrane K^+ current and migration in MDCKII cells. Therefore Ca^{2+}-activated K^+ channels play a role in HGF/SF-stimulated MDCKII cell migration. However, the cellular mechanism of Ca^{2+}-activated K^+ channel involvement is unknown. Met and/or HGF/SF expression and over-expression have been observed in a variety of tumors. HGF/SF-stimulated cell migration plays an important role in tumor invasiveness and metastasis. Therefore, the dependence of HGF/SF-stimulated migration on Ca^{2+}-activated K^+ channels may provide a locus on the cell surface for therapeutic intervention for diseases, in which cell migration contributes to the pathology.

The authors thank G.F. Vande Woude and L.-M. Wang for providing HGF/SF and MDCK II cells. This work was supported by a grant from the Eagles Kidney Foundation.

References

Baffy, G., Yang, L., Michaloopoulos, G.K., Williamson, J.R. 1992. Hepotocyte growth factor induces calcium mobilization and inositol phosphate production in rat hepatocytes. *J. Cell Physiol.* **153:**332–339

Bootman, M.D., Lipp, P., Berridge, M.J. 2001. The organisation and functions of local Ca^{2+} signals. *J. Cell Sci.* **114:**2213–2222

Cantiello, H.F., Prat, A.G., Bonventre, J.V., Cunningham, C.C., Hartwig, J.H., Ausiello, D.A. 1993. Actin-binding protein contributes to cell volume regulatory ion channel activation in melanoma cells. *J. Biol. Chem.* **268:**4596–4599

Cao, B., Su, Y., Oskarsson, M., Zhao, P., Kort, E.J., Fisher, R.J., Wang, L.-M., Vande Woude, G.F. 2001. Neutralizing monoclonal antibodies to hepatocyte growth factor/scatter factor (HGF/SF) display antitumor activity in animal models. *Proc. Natl. Acad. Sci. USA* **98:**7443–7448

Furge, K.A., Kiewlich, D., Le, P., Vo, M.N., Faure, M., Howlett, A.R., Lipson, K.E., Vande Woude, G.F., Webb, C.P. 2001. Suppression of Ras-mediated tumorigenicity and metastasis through inhibition of the Met receptor tyrosine kinase. *Proc. Natl. Acad. Sci. USA* **98:**10722–10727

Gulati, R., Peluso, J.J. 1997. Opposing actions of hepatocyte growth factor and basic fibroblast growth factor on cell contact, intracellular free calcium levels, and rat ovarian surface epithelial cell viability. *Endocrinology* **138:**1847–1856

Hamill, O.P., Marty, A., Neher, E., Sakmann, B., Sigworth, F.J. 1981. Improved patch-clamp techniques for high-resolution current recording from cells and cell-free membrane patches. *Pfluegers Arch.* **39:**85–100

Hille, B. 2001. Ion Channels of Excitable Membranes, pp. 143–147. Sinauer Assoc., Inc. Sunderland, MA

Ishii, T.M., Silvia, C., Hirschberg, B., Bond, C.T., Adelman, J.P., Maylie, J. 1997. A human intermediate conductance calcium-activated potassium channel. *Proc. Natl. Acad. Sci. USA* **94:**11651–11656

Jeffers, M., Rong, S., Anver, M., Vande Woude, G.F. 1996. Autocrine hepatocyte growth factor/scatter factor-Met signaling induces transformation and invasive/metastatic phenotype in C127 cells. *Oncogene* **13:**853–856

Jeffers, M., Rong, S., Vande Woude, G.F. 1996a. Enhanced tumorigenicity and invasion-metastasis by hepatocyte growth factor/scatter factor-met signaling in human cells concomitant with induction of the urokinase proteolysis network. *Mol. Cell. Biol.* **16:**1115–1125

Jeffers, M., Rong, S., Vande Woude, G.F. 1996b. Hepatocyte growth factor/scatter factor-Met signaling in tumorigenicity and invasion/metastasis. *J. Mol. Med.* **74:**505–513

Jensen, B.S., Strøbæk, D., Christophersen, P., Jørgensen, T.D., Hansen, C., Silahtaroglu, A., Olesen, S.-P, Ahring, P.K. 1998. Characterization of the cloned human intermediate-conductance Ca^{2+}-activated K^+ channel. *Am. J. Physiol.* **275:**C848–C856

Kaneko, A., Hayashi, N., Tsubouchi, H., Tanaka, Y., Ito, T., Sasaki, Y., Fusamoto, H., Daikuhara, Y., Kamada, T. 1992. Intracellular calcium as a second messenger for human hepatocyte growth factor in hepatocytes. *Hepatology* **15:**1173–1178

Kawanishi, T., Kato, T., Asoh, H., Uneyama, C., Toyoda, K., Momose, K., Takahashi, M., Hayashi, Y. 1995. Hepatocyte growth factor-induced calcium waves in hepatocyte as revealed with rapid scanning confocal microscopy. *Cell Calcium* **18:**495–504

Khwaja, A., Lehmann, K., Marte, B.M., Downward, J. 1998. Phosphoinositide 3-kinase induces scattering and tubulogenesis in epithelial cells through a novel pathway. *J. Biol. Chem.* **273:**18793–18801

Kidd, J.F., Fogarty, K.E., Tuft, R.A., Thorn, P. 1999. The role of Ca^{2+} feedback in shaping $InsP_3$-evoked Ca^{2+} signals in mouse pancreatic acinar cells. *J. Physiol.* **520:**187–201

Liu, S.I., Chi, C.W., Lui, W.Y., Mok, K.T., Wu, C.W., Wu, S.N. 1998. Correlation of hepatocyte growth factor-induced proliferation and calcium-activated potassium current in human gastric cancer cells. *Biochim. Biophys. Acta* **1368:**256–266

Matsumoto, K., Nakamura, T. 1996. Emerging multipotent aspects of hepatocyte growth factor. *J. Biochem.* **119:**591–600

Matsumoto, K., Nakamura, T. 1997. Hepatocyte growth factor (HGF) as a tissue organizer for organogenesis and regeneration. *Biochem. Biophys. Res. Commun.* **239:**639–644

Montesano, R., Soriano, J.V., Pepper, M.S., Orci, L. 1997. Induction of epithelial branching tubulogenesis in vitro. *J. Cell. Physiol.* **173:**152–161

Neher, E. 1998. Vesicle pools and Ca^{2+} microdomains: new tools for understanding their roles in neurotransmitter release. *Neuron* **20:**389–399

Osada, S., Saji, S., Nakamura, T., Nozawa, Y. 1992. Cytosolic calcium oscillations induced by hepatocyte growth factor (HGF) in single fura-2-loaded cultured hepatocytes: effects of extracellular calcium and protein kinase C. *Biochim. Biophys. Acta* **1135:**229–232

Pasantes-Morales, H., Morales-Mulia, S. 2000. Influence of calcium on regulatory volume decrease: role of potassium channels. *Nephron* **86:**414–427

Peluso, J.J. 1997. Putative mechanism through which N-cadherin-mediated cell contact maintains calcium homeostasis and thereby prevents ovarian cells from undergoing apoptosis. *Biochem. Pharmacol.* **54:**847–853

Pérez, G.J., Bonev, A.D., Nelson, M.T. 2001. Micromolar Ca^{2+} from sparks activates Ca^{2+}-sensitive K^+ channels in rat cerebral artery smooth muscle. *Am. J. Physiol.* **281:**C1769–C1775

Pozo, M.J., Pérez, G.J., Nelson, M.T., Mawe, G.M. 2002. Ca^{2+} sparks and BK currents in gallbladder myocytes: role in CCK-induced response. *Am. J. Physiol.* **282:**G165–G174

Rae, J., Levis, R. 2000. R-6101, an electrode coating elastomer to replace sylgard 184. *AxoBits* **29:**6–7

Royal, I., Park, M. 1995. Hepatocyte growth factor-induced scatter of Mardin-Darby canine kidney cells requires phosphatidylinositol 3-kinase. *J. Biol. Chem.* **270:**27780–27787

Schneider, S.W., Pagel, P., Rotsch, C., Danker, T., Oberleithner, H., Radmacher, M., Schwab, A. 2000. Volume dynamics in migrating epithelial cells measured with atomic force microscopy. *Pfluegers Arch.* **439:**297–303

Schwab, A. 2001. Ion channels and transporters on the move. *News Physiol. Sci.* **16:**29–33

Schwab, A., Finsterwalder, F., Kersting, U., Danker, T., Oberleithner, H. 1997. Intracellular Ca^{2+} distribution in migrating transformed renal epithelial cells. *Pfluegers Arch.* **434:**70–76

Schwab, A., Gabriel, K., Finsterwalder, F., Folprecht, G., Greger, R., Kramer, A., Oberleithner, H. 1995. Polarized ion transport during migration of transformed Madin-Darby canine kidney cells. *Pfluegers Arch.* **430:**802–807

Schwab, A., Oberleithner, H. 1996. Plasticity of renal epithelial cells: the way a potasium channel supports migration. *Pfluegers Arch.* **432:**R87–93

Schwab, A., Westphale, H.J., Wojnowski, L., Wünsch, S., Oberleithner, H. 1993. Spontaneously oscillating K^+ channels in alkali-transformed MDCK cells. *J. Clin. Invest.* **92:**218–223

Schwab, A., Wojnowski, L., Gabriel, K., Oberleithner, H. 1994. Oscillating activity of a Ca^{2+}-sensitive K^+ channel. A prerequisite for migration of transformed Madin-Darby canine kidney focus cells. *J. Clin. Invest.* **93:**1631–1636

Spitzer, N.C., Lautermilch, N.J., Smith, R.D., Gomez, T.M. 2000. Coding of neuronal differentiation by calcium transients. *BioEssays* **22:**811–817

Terauchi, R., Kitamura, N. 2000. Requirement of regulated activation of Ras for response of MDCK cells to hepatocyte growth factor/scatter factor. *Exp. Cell Res.* **256:**411–422

Trusolino, L., Cavassa, S., Angelini, P., Ando, M., Bertotti, A, Comoglio, P.M., Boccaccio, C. 2000. HGF/SF selectively promotes cell invasion by increasing integrin avidity. *FASEB J.* **14:**1629–1640

Zhuge, R., Fogarty, K.E., Tuft, R.A., Lifshitz, L.M., Sayar, K., Walsh, J.V. Jr. 2000. Dynamics of signaling between Ca^{2+}-activated K^+ channels studied with a novel image-based method for direct intracellular measurements of ryanodine receptor Ca^{2+} current. *J. Gen. Physiol.* **116:**845–864.